Empirical relations between rock strength and physical properties in sedimentary rocks

Chandong Chang [a,*], Mark D. Zoback [a,1], Abbas Khaksar [b,2]

[a] *Department of Geophysics, Stanford University, Palo Alto, CA 94305-2215, USA*
[b] *GeoMechanics International, Inc., Perth, WA 6000, Australia*

Abstract

In this study, 31 empirical equations are summarized that relate unconfined compressive strength and internal friction angle of sedimentary rocks (sandstone, shale, and limestone and dolomite) to physical properties (such as velocity, modulus, and porosity). These equations can be used to estimate rock strength from parameters measurable with geophysical well logs. The ability of these equations to fit laboratory-measured strength and physical property data that were compiled from the literature is reviewed. Results from this study can be useful for petroleum industry when a range of geomechanical problems such as wellbore stability and in-situ stress measurements should be addressed without direct strength information available. While some equations work reasonably well (for example, some strength–porosity relationships for sandstone and shale), rock strength variations with individual physical property measurements scatter considerably, indicating that most of the empirical equations are not sufficiently generic to fit all the data published on rock strength and physical properties. This emphasizes the importance of local calibration before one utilizes any of the empirical relationships presented. Nonetheless, some reasonable correlations can be found between geophysical properties and rock strength that can be useful for applications related to wellbore stability where having a lower bound estimate of in situ rock strength is especially useful.
© 2006 Elsevier B.V. All rights reserved.

1. Introduction

The unconfined compressive strength (UCS) and angle of internal friction (Φ) of sedimentary rocks are key parameters needed to address a range of geomechanical problems ranging from limiting wellbore instabilities during drilling (e.g. Moos et al., 2003), to assessing sanding potential (e.g. Santarelli et al., 1989) and quantitatively constraining stress magnitudes using observations of wellbore failure (e.g. Zoback et al., 2003). Laboratory-based UCS and Φ are typically determined through triaxial tests on cylindrical samples that are obtained from depths of interest. In practice, however, many geomechanical problems in reservoirs must be addressed when core samples are unavailable for laboratory testing. In fact, core samples of overburden formations (where many wellbore instability problems are encountered) are almost never available for testing.

* Corresponding author. Now at: Chungnam National University, Daejeon 305-764, South Korea. Fax: +82 42 823 5636.
  E-mail addresses: cchang@cnu.ac.kr (C. Chang),
zoback@pangea.stanford.edu (M.D. Zoback),
abbas.khaksar@helix-rds.com (A. Khaksar).
[1] Fax: +1 650 725 7344.
[2] Now at: Helix RDS Ltd., Perth, WA 6000, Australia. Fax: +61 8 9322 9833.

As a practical approach to these problems, a number of empirical relations have been proposed that relate rock strength to parameters measurable with geophysical well logs. The use of such relations is often the only way to estimate strength in many situations due to the absence of cores for laboratory tests. The basis for these relations is the fact that many of the same factors that affect rock strength also affect other physical properties such as velocity, elastic moduli and porosity. In many cases, such relationships have been suggested for sedimentary rocks mainly because the strength information is greatly demanded in reservoirs for drilling and maintenance of wellbores.

In general, a strength–physical property relationship for a specific rock formation is developed based on calibration through laboratory tests on rock cores from the given field. If there are no core samples available for calibration, the next best thing would be to use empirical strength relations based on measurable physical properties. Because there are multiple choices of strength models for various rock types in different geological settings, it is necessary to understand the characteristics of the models and their range of applicability prior to utilizing them. In order to review the suitability of existing strength relations for various sedimentary rocks (sandstone, shale, and carbonate rocks), 31 different empirical relations (both published and proprietary) are summarized and compared with an extensive dataset of published laboratory-determined rock physical/mechanical properties. The goal of this review is to synthesize and compare the many relations proposed over the years and provide insight into the appropriateness of the various proposed criteria for rock strength when no core samples are available for testing.

2. Physical/mechanical property data for sedimentary rocks

Nearly all proposed formulae for determination of rock strength from geophysical logs utilize one (or more) of the following parameters:

- P-wave velocity (V_p), or equivalently, interval transit time ($\Delta t = V_p^{-1}$), which is directly measured,
- Young's modulus (E), which is derived from velocity and density measurements, or
- Porosity (ϕ), which is usually derived from density measurements assuming rock matrix and fluid densities.

Conceptually, the justification for the empirical relations discussed below is the general correlation between these parameters and unconfined compressive strength. These general correlations are seen in the laboratory data presented in Figs. 1–3 for sandstone, shale, and limestone and dolomite, respectively. Despite the considerable scatter in the data, for each rock type, there is a marked decrease in strength with Δt and ϕ,
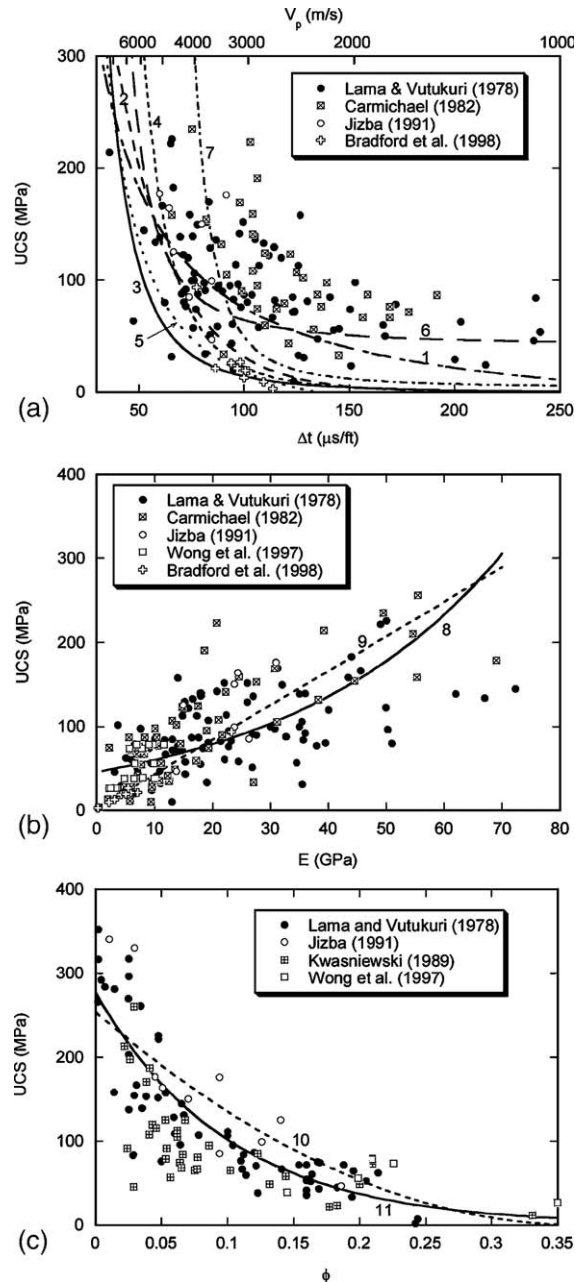

Fig. 1. Comparison between different empirical equations listed in Table 1 for the dependence of the strength of 260 sandstones on (a) interval transit time (or equivalently P-wave velocity), (b) Young's modulus, and (c) porosity. Note that Δt is for dry conditions.
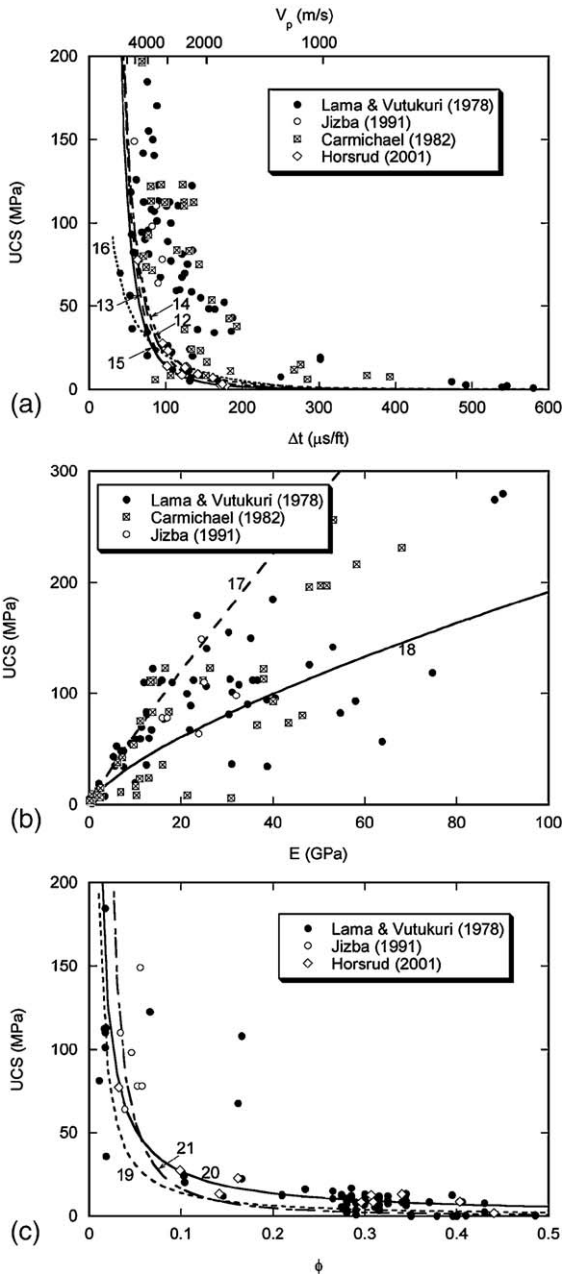
Fig. 2. Comparison between different empirical equations listed in Table 2 for the dependence of the strength of 100 shales on (a) interval transit time (or equivalently P-wave velocity), (b) Young's modulus, and (c) porosity. Note that Δt is for dry conditions, except those from Horsrud (2001).

and an increase in strength with E. The unit of µs/ft is used for Δt here because it is much more frequently used in the petroleum industry than SI unit. The rock strength and physical property data presented in these figures were compiled from the literature (Lama and Vutukuri, 1978; Carmichael, 1982; Kwasniewski, 1989;

Jizba, 1991; Wong et al., 1997; Bradford et al., 1998; Horsrud, 2001—see symbols). Lama and Vutukuri (1978) and Carmichael (1982) tabulated extensive lists of various mechanical properties of sedimentary rocks from different locations around the world. Kwasniewski (1989) listed UCS and porosity data of various
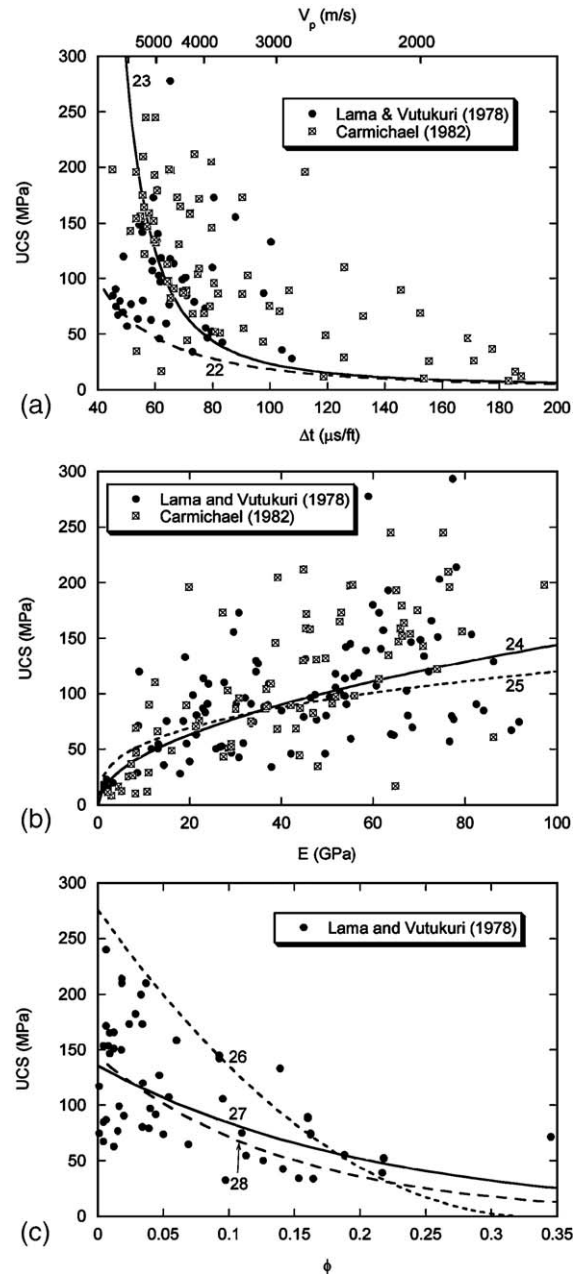

Fig. 3. Comparison between different empirical equations listed in Table 3 for the dependence of the strength of 140 limestones and dolomites on (a) interval transit time (or equivalently P-wave velocity), (b) Young's modulus, and (c) porosity. Note that Δt is for dry conditions.

sandstones. Jizba (1991) presented mechanical properties of sandstones and shales with a wide range of porosity recovered from different depths in a borehole in Texas, USA. Wong et al. (1997) presented a table of strength and other physical properties of several representative porous sandstones. Bradford et al. (1998) and Horsrud (2001) reported laboratory test results on the North Sea sandstone and shale, respectively. The compiled data constitute a database of about 260 sandstones, 100 shales, and 140 limestones and dolomites.

Although the overall quality of the laboratory strength and physical property data we utilize in this study is an important issue, it is beyond the scope of this work (and essentially impossible) to validate how each data point was measured in the laboratory. For instance, the measure of static Young's modulus varies depending on loading/unloading path and the level of confining pressure (Plona and Cook, 1995). Velocities are also stress-dependent (Johnston and Toksöz, 1980; Mashinskii, 2004). Unconfined compressive strength can be determined either through direct measurement from uniaxially loaded samples, or through an indirect estimation from a series of triaxial tests, which usually results in some difference in UCS. All these can cause the scatter of the data.

The majority of laboratory-measured data collected were static measurements (i.e. static E instead of dynamic E). A limited number of dynamic measurement data (i.e. velocity measurements) were available in some source (Carmichael, 1982; Jizba, 1991; Bradford et al., 1998; Horsrud, 2001). Because of the paucity of data, Δt was derived from static Young's modulus (along with Poisson's ratio and dry density) except those directly available. The use of the static moduli to compute the interval transit time generally yields Δt values higher than those from actual velocity measurements because of frequency-dependence of moduli (Biot, 1956; Mavko and Nur, 1979). Previous measurements generally indicate that dynamic modulus in dry rock is similar to, or higher than (roughly up to twice depending on rock types), the static modulus (Rzhevsky and Novick, 1971; Ramana and Venkatanarayana, 1973; Cheng and Johnston, 1981; Fjaer, 1999). The main factor that causes the frequency-dependence of moduli is the presence of pore fluid trapped in rock and its frequency-dependent mobility during rock deformation such that these phenomena should be relatively insignificant in dry rock. A recent experimental study showed that frequency has little effect on velocity in dry sandstone over a frequency band of 10–10^6 Hz, a frequency band that covers static to ultrasonic range (Batzle et al., 2001). Since Δt is in proportion to $E^{-0.5}$,

the use of static modulus instead of dynamic equivalent has an even less significant impact on Δt values. As all the laboratory-measured static data used to calculate Δt are measurements on dry rocks, the effect of modulus dispersion (i.e. difference between static and dynamic) should be minor. This issue will be dealt with briefly in the Discussion.

Because of the considerable scatter in the data presented in Figs. 1–3, it is impossible for any single relationship to fit all of the data shown. In the sections below, the ability of each equation to fit the data is quantitatively analyzed by comparing the difference between each model's estimated UCS (UCS_E) and measured UCS data (UCS_M) for a given measured physical property. The obtained values of [$UCS_E - UCS_M$] were then used to construct histograms showing a percentage frequency distribution as a function of [$UCS_E - UCS_M$]. This was carried out for two ranges of values of each parameter (i.e. low and high ranges of values for V_p, E, ϕ) to test whether individual models are more suitable for a particular range of parameter.

3. Empirical strength equations for sedimentary rocks

3.1. Sandstones

Eqs. (1)–(11) in Table 1 present a number of relationships in common practice (both published and proprietary) for estimating the unconfined compressive strength of sandstones from geophysical logging data. These relations were derived for case studies carried out for markedly different rocks in markedly different geological settings, around the world. To the degree possible, general comments such as the regions and/or the general rock properties appropriate for each equation were indicated in Table 1. If no reference is shown, the given empirical relation is unpublished. Eqs. (1)–(3) utilize V_p (or expressed equivalently as Δt) measurements from well logs. Eqs. (5)–(7) utilize both density and V_p data, and Eq. (4) utilizes V_p, density ρ, Poisson's ratio v (which requires V_s measurements) and clay volume V_{clay} (from gamma ray logs). Eqs. (8) and (9) utilize Young's modulus, E, derived from V_p, V_s, ρ, and Eqs. (10) and (11) utilize log-derived porosity measurements to estimate UCS.

In order to compare the various velocity-based strength models (Eqs. (1)–(7)) in a single UCS–Δt domain (Fig. 1a), it was required to estimate ρ, v and V_{clay} in Eqs. (4)–(7) to isolate Δt (or V_p) as the only independent variable. Constant values of ρ ($=2.3$ g/cm^3)

Table 1
Empirical relationships between unconfined compressive strength (UCS) and other physical properties in sandstone

Eq. no.	UCS (MPa)	Region where developed	General comments	Reference
(1)	$0.035V_p - 31.5$	Thuringia, Germany	–	Freyburg (1972)
(2)	$1200\exp(-0.036\Delta t)$	Bowen Basin, Australia	Fine grained, both consolidated and unconsolidated sandstones with all porosity range	McNally (1987)
(3)	$1.4138 \times 10^7 \Delta t^{-3}$	Gulf Coast	Weak and unconsolidated sandstones	
(4)	$3.3 \times 10^{-20} \rho^2 V_p^4 \, [(1+v)/(1-v)]^2(1-2v) \, [1+0.78V_{clay}]$	Gulf Coast	Applicable to sandstones with UCS > 30 MPa	Fjaer et al. (1992)
(5)	$1.745 \times 10^{-9} \rho V_p^2 - 21$	Cook Inlet, Alaska	Coarse grained sandstones and conglomerates	Moos et al. (1999)
(6)	$42.1\exp(1.9 \times 10^{-11} \rho V_p^2)$	Australia	Consolidated sandstones with $0.05 < \phi < 0.12$ and UCS > 80 MPa	
(7)	$3.87\exp(1.14 \times 10^{-10} \rho V_p^2)$	Gulf of Mexico	–	
(8)	$46.2\exp(0.027E)$	–	–	
(9)	$2.28 + 4.1089E$	Worldwide	–	Bradford et al. (1998)
(10)	$254 \, (1 - 2.7\phi)^2$	Sedimentary basins worldwide	Very clean, well-consolidated sandstones with $\phi < 0.3$	Vernik et al. (1993)
(11)	$277\exp(-10\phi)$	–	Sandstones with 2 < UCS < 360 MPa and $0.002 < \phi < 0.33$	

and v (=0.21), and zero clay volume were used as appropriate. As these are reasonable average values of sandstones, using these constants will obviously result in some misfit for some specific samples, but will hopefully not cause any systematic misfits when considering all of the samples tested.

The first impression one gets from seeing the fit between the measured strength and velocity data in the laboratory with the seven empirical relations appropriate for the UCS–Δt domain in Fig. 1a is that the scatter is remarkably large–a roughly ~100 MPa variation of strength–at any given Δt. Except for Eqs. (1) and (6) (derived for relatively strong rocks), all of the relations appear to badly underpredict the strength data for high travel times ($\Delta t > 100 \, \mu s/ft$), or very low velocities ($V_p < 3000 \, m/s$). Such velocities are characteristic of very weak sandstones such as found in the Gulf of Mexico (GOM), but one needs to keep in mind that there are essentially no very weak sands represented in most of the strength data available except those provided by Bradford et al. (1998). Similarly, for fast, high strength rocks, Eq. (3) (derived for low strength rocks) does a particularly poor job of fitting the data. The overall misfits between the expected unconfined compressive strength (UCS$_E$) and measured values (USC$_M$) are summarized in Fig. 4a and b for relatively fast and slow rocks, respectively.

The estimated strengths from Eqs. (2)–(5) and (7) are very similar to one another for high travel time (Δt higher than about 120 $\mu s/ft$) sandstones (Fig. 1a) as most of these equations are derived for the GOM or Gulf Coast sandstone (Table 1). The variation of rock

strength estimated using these relations is within 10 MPa. Fig. 1a also shows that the data of the very weak North Sea sandstone provided by Bradford et al. (1998) are fairly well fitted by Eqs. (3), (4) and (5) and very close to Eqs. (2) and (7). These suggest that the rock strength of very weak sandstones from the GOM, the North Sea, and probably other sedimentary basins are characterized by a similar strength–velocity trend.

The use of Young's modulus for estimating UCS is less straightforward than that of velocity, because it generally requires the static–dynamic conversion or frequency correction. Young's modulus data in Fig. 1b (Figs. 2b and 3b as well) are all static measurements. Eqs. (8) and (9) derived using static Young's modulus fit the available data shown in Fig. 1b reasonably well in the lower E range, fitting 60% and 54%, respectively, of the given data within ±30 MPa (Fig. 4c). Fig. 4c and d show that mean [UCS$_E$ – UCS$_M$] for Eq. (8) is around zero, indicating this relation passes through the average of most of the strength data. Eq. (9) tends to underestimate strength at low E and overestimate strength at high E; however, there is considerable scatter at any given value of E (Fig. 1b).

With respect to porosity, both of the porosity relations listed in Table 1 seem to generally overestimate strength, except for the very lowest porosities. The histogram of misfits shows that Eq. (11) predicts UCS fairly well for high porosities (>0.1), fitting 29% of data within ±10 MPa and 80% of data within ±30 MPa (Fig. 4f). Eq. (10) lies along the upper bound of UCS data, overestimating sandstone strength. Eq. (10) was derived for very clean and well-consolidated sandstones, and
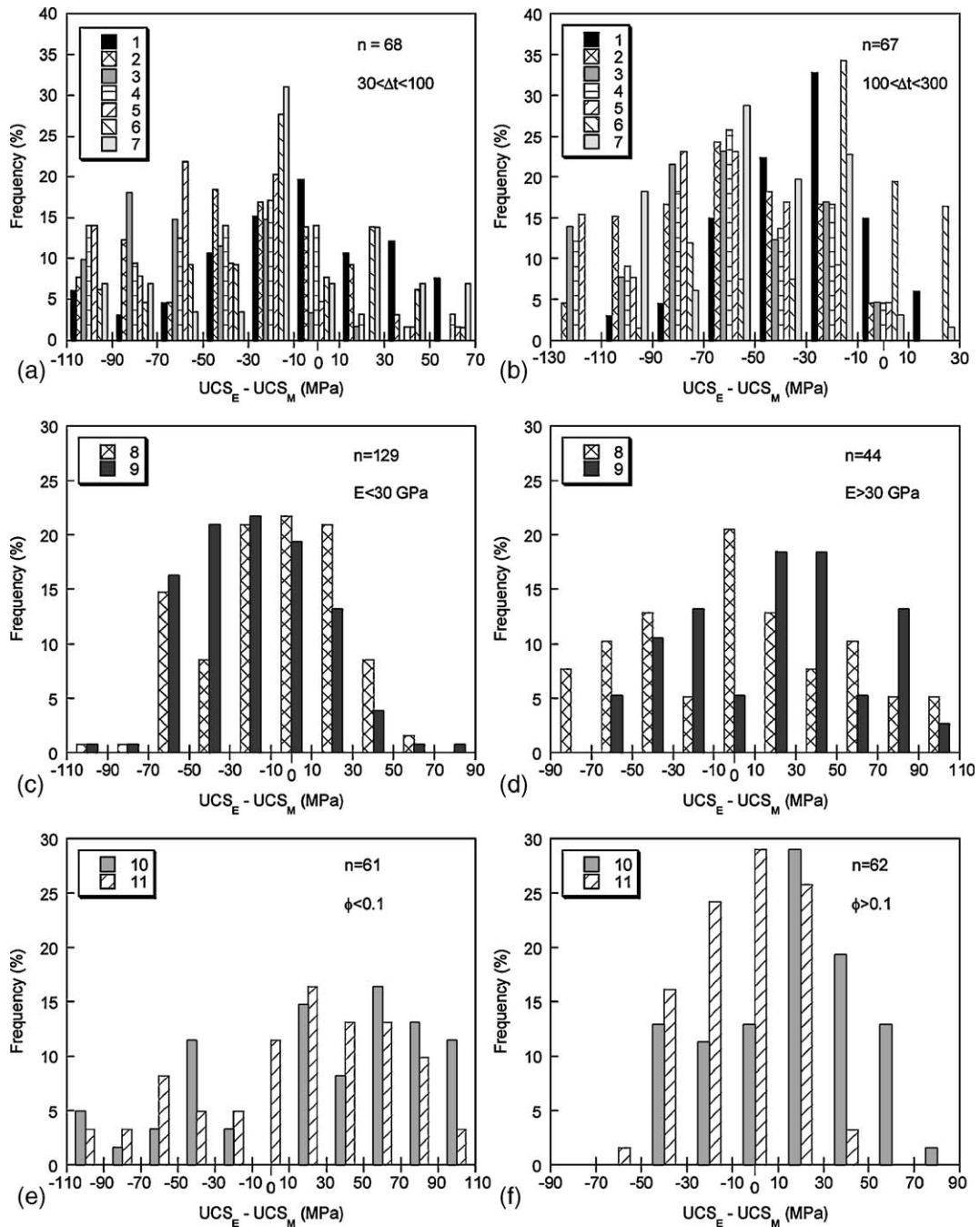
Fig. 4. Histograms showing frequency versus difference in estimated unconfined compressive strength (UCS_E) and measured unconfined compressive strength (UCS_M) in sandstones using different empirical equations shown in Table 1. For each given parameter, lower and upper ranges were analyzed separately. Numbers in legend indicate equation numbers. The value of n denotes the number of data.

should not be used to estimate UCS of sands with porosity higher than 0.37, where the predicted UCS starts to increase as porosity increases. Thus, care should be taken when Eq. (10) is used to estimate UCS of high porosity unconsolidated sandstones, typical of sea floor soft sediments. An extremely wide range of

UCS (a range of ∼300 MPa) is observed in the data at $\phi < 0.05$ (Fig. 1c). This suggests that porosity alone is not a good indicator for strength of low porosity sandstone. Such a wide scatter in rock strength can be attributed to different diagenetic processes (e.g. quartz vs. calcite cement, etc.) as sandstones are compacted.

Overall, none of the equations in Table 1 do a very good job of fitting the data in Fig. 1. The validity of any of these relations is best judged in terms of how well it would work for the rocks for which they were originally derived. Thus, calibration is extremely important before utilizing any of the relations shown. Eq. (5), for example, seems to systematically underpredict most of the data in Fig. 1a, yet worked very well for the relatively clean sands from the North Sea (Bradford et al., 1998) since it was derived for an equivalently clean coarse-grained sandstone (Moos et al., 1999).

3.2. Shales

The empirical relations for the strength of shale listed in Table 2 are based on model calibration for unconsolidated porous shales of Tertiary, or younger age except for Eqs. (18) and (19) developed for rather strong shales. Note that Eqs. (12)–(15), principally utilizing Δt for UCS estimation, are expressed in the same form of power law function of Δt with slightly different coefficients and exponents. These equations show nearly the same trends, providing a lower bound of the data (Fig. 2a). As mentioned above, it is prudent to underestimate strength to be conservative for applications to wellbore stability. The difference between these relations and the measured strengths is quite marked for fast, low Δt, rocks. In the low Δt range (<100), more than 80% of UCS data are higher by 30–90 MPa than the estimated values from Eqs. (12)–(16). For slower rocks ($\Delta t > 100$), these equations fit about 30–35% of data within ±10 MPa. Still almost all data are located above the model predictions, implying that the UCS–Δt relationships provide only a lower bound of UCS of shale. Eqs. (12)–(16) were calibrated for samples collected from the North Sea and Gulf of Mexico where high porosity, unconsolidated Tertiary or younger shales are dominant, while

the majority of rock strength data presented in Fig. 2a came from shales that underwent a higher degree of diagenesis except for the North Sea shale (Horsrud, 2001). Thus, the use of the empirical equations leads to significant misfits in most cases, while estimating the North Sea shale data fairly well. Note in Fig. 5b that the strengths of the majority of slow, weak shales are either fit well, or underestimated by relations (12)–(16). Hence, such relations form a useful, if perhaps overly conservative, means for estimating shale strength in weak formations.

The two relations (Eqs. (17) and (18)) that utilize Young's modulus for estimating UCS show a remarkable difference in their general trends (Fig. 2b). This is because the two equations were developed based on markedly different rock types: Eq. (17) was developed for high porosity North Sea shale and Eq. (18) from relatively strong compacted shale. Perhaps the only conclusion that can be reached from this comparison is that Eq. (17) appears to predict shale strength in the lower E range (<30 GPa) fairly well, fitting 75% of the given data within ±30 MPa (Fig. 5c), while it considerably overestimates strength for rocks with higher E. In contrast, Eq. (18) fits 45% of the data in the higher E within ±30 MPa (Fig. 5d), even though a wide scatter in data inhibits a reasonable fitting.

Eqs. (19)–(21) that utilize porosity are in a similar form of power law function and exhibit a similar decreasing trend of UCS as a function of ϕ (Fig. 2c). Unlike the case for sandstones, porosity appears to be a good parameter that can be used to estimate UCS of shale, especially for high porosities (>0.1). The three Eqs. (19)–(21) all predict shale strength fairly well, fitting 90% of available data within ±10 MPa (Fig. 5f). This is a very useful result since the weak shales are major constituents of most sedimentary basins and reservoir that often cause major wellbore stability problems. Their strength can be relatively

Table 2
Empirical relationships between unconfined compressive strength (UCS) and other physical properties in shale

| Eq. no.	UCS (MPa)	Region where developed	General comments	Reference
(12)	$0.77 (304.8/\Delta t)^{2.93}$	North Sea	Mostly high porosity Tertiary shales	Horsrud (2001)
(13)	$0.43 (304.8/\Delta t)^{3.2}$	Gulf of Mexico	Pliocene and younger	
(14)	$1.35 (304.8/\Delta t)^{2.6}$	Globally	–	
(15)	$0.5 (304.8/\Delta t)^{3}$	Gulf of Mexico	–	
(16)	$10 (304.8/\Delta t - 1)$	North Sea	Mostly high porosity Tertiary shales	Lal (1999)
(17)	$7.97 E^{0.91}$	North Sea	Mostly high porosity Tertiary shales	Horsrud (2001)
(18)	$7.22 E^{0.712}$	–	Strong and compacted shales	
(19)	$1.001 \phi^{-1.143}$	–	Low porosity ($\phi < 0.1$) high strength (~ 79 MPa) shales	Lashkaripour and Dusseault (1993)
(20)	$2.922 \phi^{-0.96}$	North Sea	Mostly high porosity Tertiary shales	Horsrud (2001)
(21)	$0.286 \phi^{-1.762}$	–	High porosity ($\phi > 0.27$) shales	
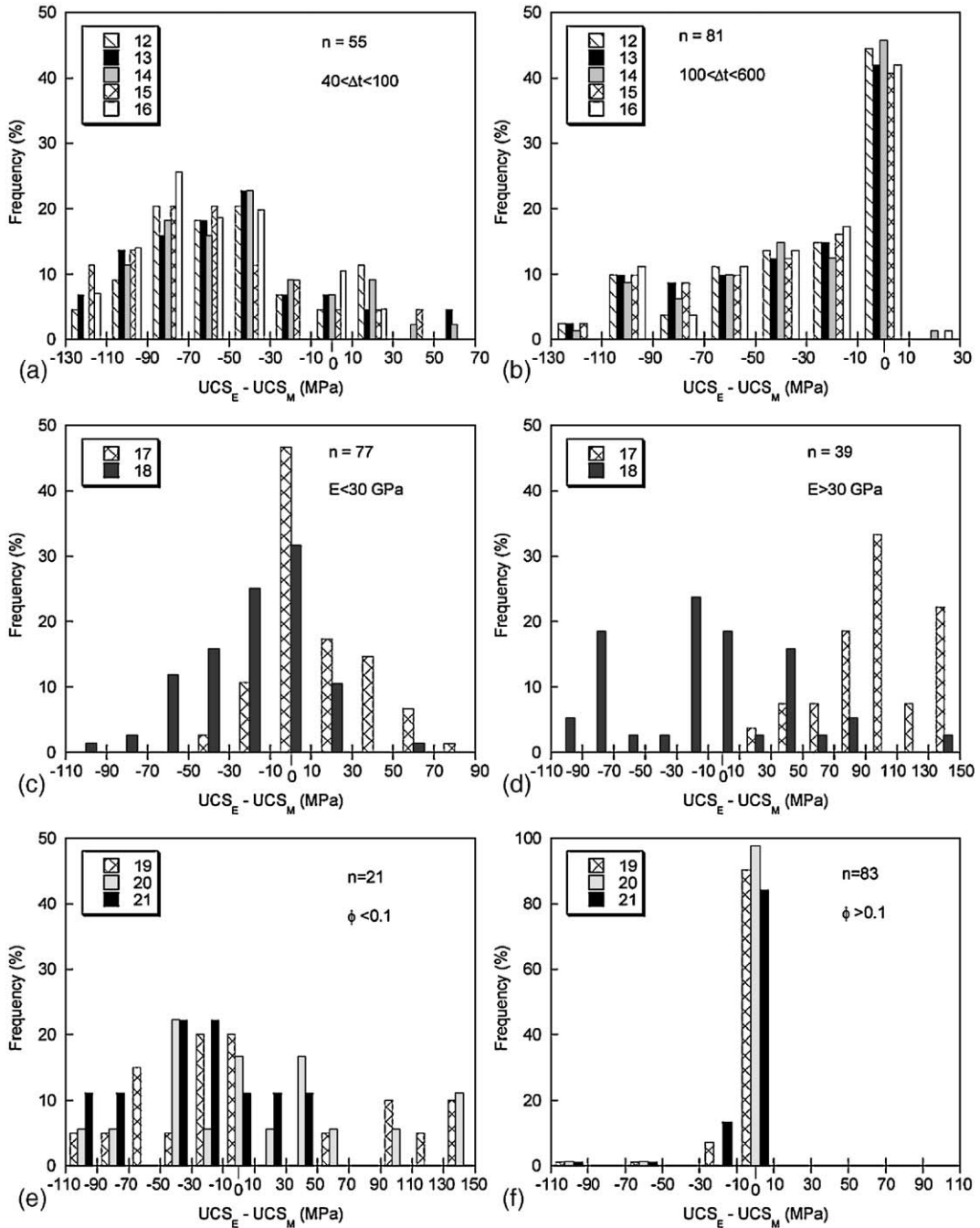
Fig. 5. Histograms showing frequency versus difference in estimated unconfined compressive strength (UCS$_E$) and measured unconfined compressive strength (UCS$_M$) in shale using different empirical equations shown in Table 2. For each given parameter, lower and upper ranges were analyzed separately. Numbers in legend indicate equation numbers. The value of n denotes the number of data.

well constrained with empirical relations that utilize porosity as a constitutive parameter. While Eqs. (19) and (21) estimate nearly the same UCS, Eq. (20) predicts slightly higher UCS (by 4 to 10 MPa) than the other two. In the lower porosity range (<0.1), the fit is

not as good but there are only a limited number of available data. Statistically, however, Eq. (19) appears to do a better job than the other two (Fig. 5e), which supports the fact that the former equation was developed based on low porosity and high strength shale.

3.3. Limestone and dolomite

Table 3 lists seven empirical equations relating the strength of limestone and dolomite to measurable geophysical parameters. Both limestone and dolomite are analyzed as one carbonate rock group as there is insufficient information to separate the relation between strength and mechanical properties for the individual rock types. Unfortunately, this results in an extraordinarily wide variation of strength of limestone and/or dolomite with any given parameter (Fig. 3). For example, at low porosity, high velocity and high stiffness, strength varies by almost a factor of four, regardless of whether uses velocity, Young's modulus or porosity to estimate strength. Thus, empirical equations relating the strength of carbonate rocks to geophysical parameters do a fairly poor job whether considering velocity, modulus or porosity data, which emphasizes the importance of being able to calibrate strength in any given case. Nevertheless, there are some meaningful points that can be extracted from Fig. 3. While Eq. (22) gives statistically less satisfactory results than Eq. (23) to all of the data (Fig. 6a and b), the former equation defines a clear lower bound of measured strength data for any given Δt (Fig. 3a). As the conservative strength estimation is important for wellbore stability problems, Eq. (22) gives a good first approximation of the lower limit of carbonate rock strength when Δt (or velocity) is known. With respect to E, both Eqs. (24) and (25) pass through the average of data set, predicting similar strength values (Figs. 3b and 6c,d). Eq. (24) gives slightly better statistical results than Eq. (25), probably because the former equation utilized a wider range of UCS data than the latter when developed. In terms of porosity, Eqs. (27) and (28) estimate average values of UCS for a given ϕ, while Eq. (26) defines an upper bound of the given data set. Thus, Eq. (26) is unfavorable at low porosities, and at porosities greater than 0.1, Eqs. (27) and (28) seem to work well.

4. Estimation of angle of internal friction

Along with the unconfined compressive strength of rock, the angle of internal friction is another strength parameter necessary to estimate rock strength at depth. Although many different failure criteria have been proposed to describe rock strength under different stress conditions based on the different types of laboratory tests (i.e. uniaxial, triaxial, and polyaxial tests), Colmenares and Zoback (2002) reviewed these criteria and discussed their fit to polyaxial rock strength data. The commonly used Mohr–Coulomb criterion has the form of

$$\sigma_1 = \text{UCS} + \sigma_3 \tan^2(45^\circ + \Phi/2) \qquad (29)$$

where Φ is a material property termed angle of internal friction (the coefficient of internal friction μ_i is defined as $\mu_i = \tan\Phi$). The angle of internal friction is a measure of the dependence of rock strength on confining pressure such that a higher value of Φ indicates a higher sensitivity of strength to confining pressure. Similarly, the Drucker and Prager criterion (1952) and the modified Lade criterion (Ewy, 1998) can also be expressed in terms of UCS and Φ (Colmenares and Zoback, 2002). Thus, if Φ can be estimated along with UCS, it is possible to construct any of the commonly used failure criteria above, which can fully define rock strength at depth.

There have been relatively few attempts to find relationships between Φ and geophysical log measurements, in part because of the fact that even weak rocks have relatively high Φ, and there are relatively complex relationships between Φ and micromechanical features of rock such as a rock's stiffness, which largely depends on cementation and porosity. In addition, there is rarely a unique value of friction angle for a rock, because the

Table 3

Empirical relationships between unconfined compressive strength (UCS) and other physical properties in limestone and dolomite

| Eq. no.	UCS (MPa)	Region where developed	General comments	Reference
(22)	$(7682/\Delta t)^{1.82}/145$	–	–	Militzer and Stoll (1973)
(23)	$10^{(2.44+109.14/\Delta t)}/145$	–	–	Golubev and Rabinovich (1976)
(24)	$13.8E^{0.51}$	–	Limestone with $10 < \text{UCS} < 300$ MPa	
(25)	$25.1E^{0.34}$	–	Dolomite with $60 < \text{UCS} < 100$ MPa	
(26)	$276(1-3\phi)^2$	Korobcheyev deposit, Russia	–	Rzhevsky and Novick (1971)
(27)	$143.8\exp(-6.95\phi)$	Middle East	Representing low to moderate porosity ($0.05 < \phi < 0.2$) and high UCS ($30 < \text{UCS} < 150$ MPa)	
(28)	$135.9\exp(-4.8\phi)$	–	Representing low to moderate porosity ($0 < \phi < 0.2$) and high UCS ($10 < \text{UCS} < 300$ MPa)	
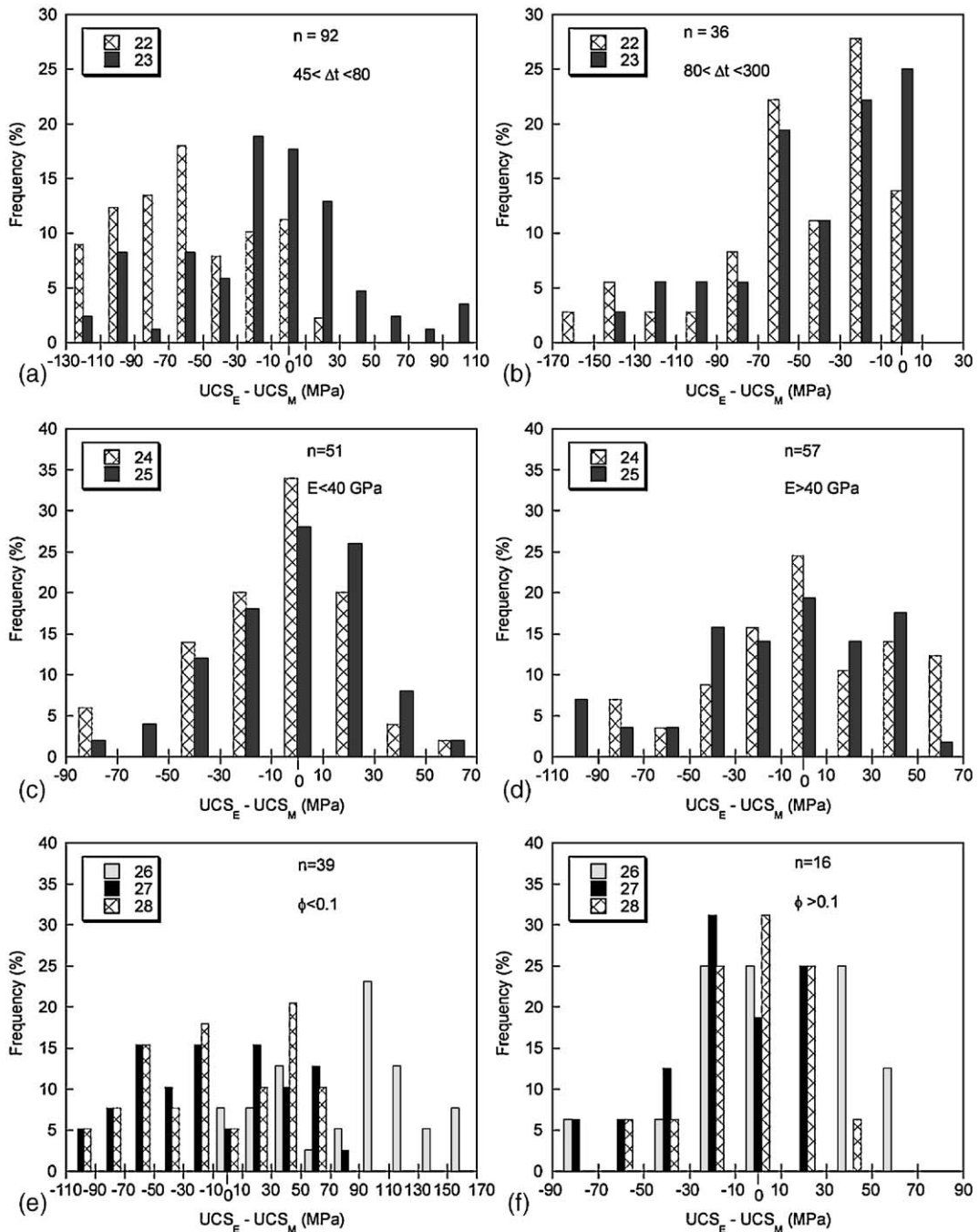
Fig. 6. Histograms showing frequency versus difference in estimated unconfined compressive strength (UCS$_E$) and measured unconfined compressive strength (UCS$_M$) in limestone and dolomite using different empirical equations shown in Table 3. For each given parameter, lower and upper ranges were analyzed separately. Numbers in legend indicate equation numbers. The value of n denotes the number of data.

strength points as a function of confining pressure are not usually linear. Friction angle depends on the confining stress range over which the data are fit. Nonetheless, some experimental evidence shows that shale with higher Young's modulus generally tends to

possess a higher Φ (Lama and Vutukuri, 1978). Three empirical equations relating Φ to rock properties for shale and sandstone are listed in Table 4.

Eq. (30) utilizes V_p to estimate the internal friction angle of shale. In Fig. 7a, Eq. (30) as well as measured

Table 4
Empirical relationships between internal friction angle (Φ) and other logged measurements

Eq. no.	Φ (degree)	General comments	Reference
(30)	$\sin^{-1}\left((V_\mathrm{p}-1000)/(V_\mathrm{p}+1000)\right)$	Shale	Lal (1999)
(31)	$57.8-105\phi$	Sandstone	Weingarten and Perkins (1995)
(32)	$\tan^{-1}\left(\dfrac{(GR-GR_\mathrm{sand})\mu_\mathrm{shale}+(GR_\mathrm{shale}-GR)\mu_\mathrm{sand}}{GR_\mathrm{shale}-GR_\mathrm{sand}}\right)$	Shaley sedimentary rocks	

shale data from the literature (Lama and Vutukuri, 1978; Carmichael, 1982) were plotted. Based on this equation, the predicted internal friction angle increases monotonically from 0° to 45° as P-wave velocity increases from 1000 m/s to 6000 m/s. The distribution of the measured internal friction angle ranges from 15° to 40° as V_p varies between 1000 and 4000 m/s range, indicating that even unconsolidated shales with low velocities have Φ values of higher than 15°. There is an increasing trend of Φ with V_p in the real data, but it is not as evident as indicated by Eq. (30). The empirical equation generally underestimates the internal friction angle for shales with V_p less than 3000 m/s, i.e. poorly consolidated or unconsolidated weak shale.

The porosity-based empirical equation (Eq. (31)) predicts Φ to decrease with increasing porosities. A limited number of published experimental data for sandstone were plotted with Eq. (31) in Fig. 7b (Handin et al., 1963; Murrell, 1965; Gowd and Rummel, 1977, Scott and Nielsen, 1991; Wong et al., 1997). Overall, the data show a fairly similar trend of Φ–porosity relation given by the empirical equation, even though there is some scatter ($\pm10°$) in Φ for a given porosity. As described below, the effect of uncertainty in the Φ value in estimating rock strength is not as significant as uncertainty in the UCS value. For example, an uncertainty of $\pm10°$ in Φ does not have a significant effect on sandstone strength estimation at elevated pressure.

Eq. (32) principally utilizes gamma ray (GR) log for the estimation of Φ value in shaley sedimentary rocks. It requires the reference GR and μ_i values for pure shale and pure sand, which are typically either assumed or determined from log-based calibration. Eq. (32) predicts the angle of internal friction that decreases gradually as GR value increases (Fig. 7c). Because GR is a measure of the amount of shale volume contained in a formation, Eq. (32) implies that a shalier rock possess a lower value of internal friction angle. No published data were

available to us to verify the reliability of the equation; however, the general trend of Φ as a function of velocity, porosity and shaliness given by Eqs. (30)–(32) are in agreement with observations made by others (Wong et al., 1993; Plumb, 1994; Horsrud, 2001).
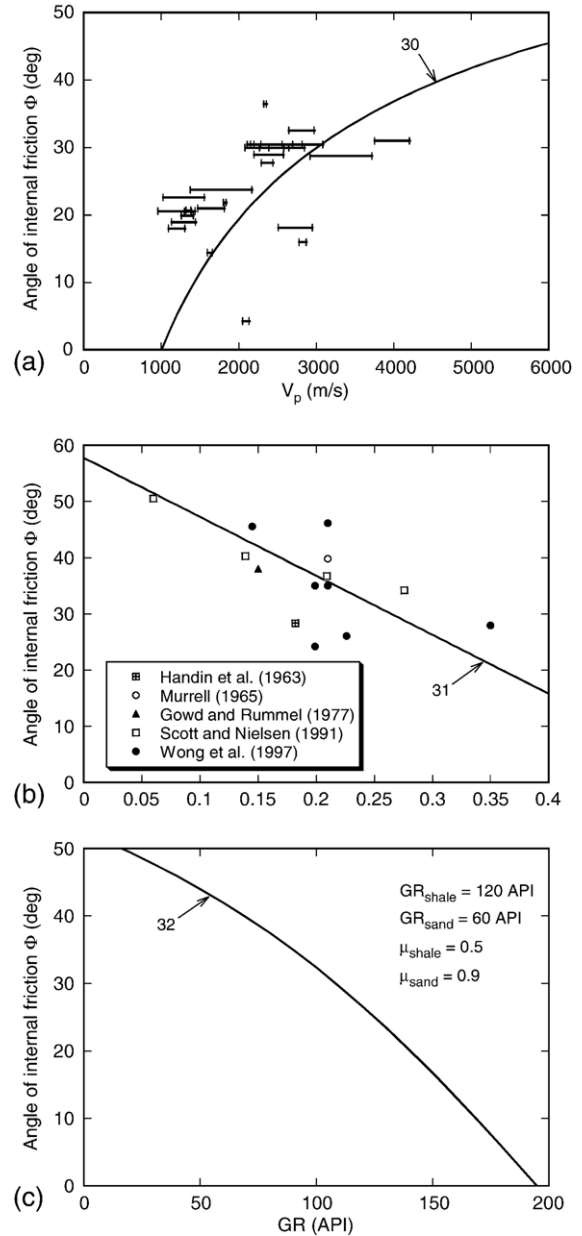

Fig. 7. Empirical equations listed in Table 4 that relate the angle of internal friction to (a) P-wave velocity, (b) porosity, and (c) gamma ray measurements. The laboratory-measured data in (a) were obtained from Lama and Vutukuri (1978) and Carmichael (1982). Data in (b) are for sandstone. The reference values of gamma ray (GR) and internal friction coefficient (μ_i) for pure sand and pure shale in (c) were assumed as indicated in the plot.

In principle, an accurate estimation of Φ is as important as that of UCS to correctly predict rock strength at depth, especially for weak rocks. Typical weak shales have a relatively narrow range of internal friction angle (roughly between 15° and 40° as shown in Fig. 7a), and the uncertainty in rock strength due to uncertain Φ value is only an order of the local least principal stress magnitude around wellbore (if the Mohr–Coulomb failure criterion is utilized for example). If the magnitude of the local least principal stress (i.e. effective borehole pressure) is considerably lower than UCS, the impact of uncertainty in Φ value on estimating in situ rock strength is minor compared to that of UCS.

5. Discussion

An example of how rock strength is determined from geophysical logs using three of the empirical relations in Table 2 is illustrated in Figs. 8 and 9 for a shale section in a vertical well in the Gulf of Mexico. The interval from 2440 to 3050 m is focused on where available logging data includes compressional wave velocity, gamma ray and density. The coefficient of internal friction was determined using the relation in terms of gamma ray described by Eq. (32) in Table 4. Although this interval is comprised of almost 100% shale, the value of μ_i ranges between 0.7 and 0.84 (corresponding to Φ between 35° and 40°). Using the velocity data, the UCS was determined using Eqs. (12) and (13) (Fig. 8a and b, respectively). While the overall shape of the two strength logs is approximately the same (as both are derived from the V_p data), the strength derived using Eq. (12) is 10.2 ±1.6 MPa (Fig. 9a), whereas that derived with Eq. (13) has a strength of 7.3±1.3 MPa (Fig. 9b). Porosity was derived from the density log assuming a matrix density of 2650 kg/m^3 and a fluid density of 1100 kg/m^3. The porosity-derived UCS is shown in Fig. 8c utilizing Eq. (20). Using this relation, the mean strength is 13.0± 1.3 MPa (Fig. 9c). There is an almost factor of two variation in mean strength. As Eq. (13) was derived for shales in the Gulf of Mexico region, however, it is probably more representative of actual strengths at depth. Again, while there are multiple options for determining strength from logs, it is best to use relations derived for formations characteristic of a particular region, and better yet, to calibrate the relation one proposes to use with laboratory measurements on representative core samples.

As mentioned earlier, the majority of the rock property data used in this study are from laboratory measurements on dry rock specimens. The applicability of the dry properties to in situ conditions may not be strictly valid, in part because rocks in the field are typically saturated with different types of fluid. Existence of fluid in pore spaces influences on bulk rock properties in many complicated ways. Saturation effect
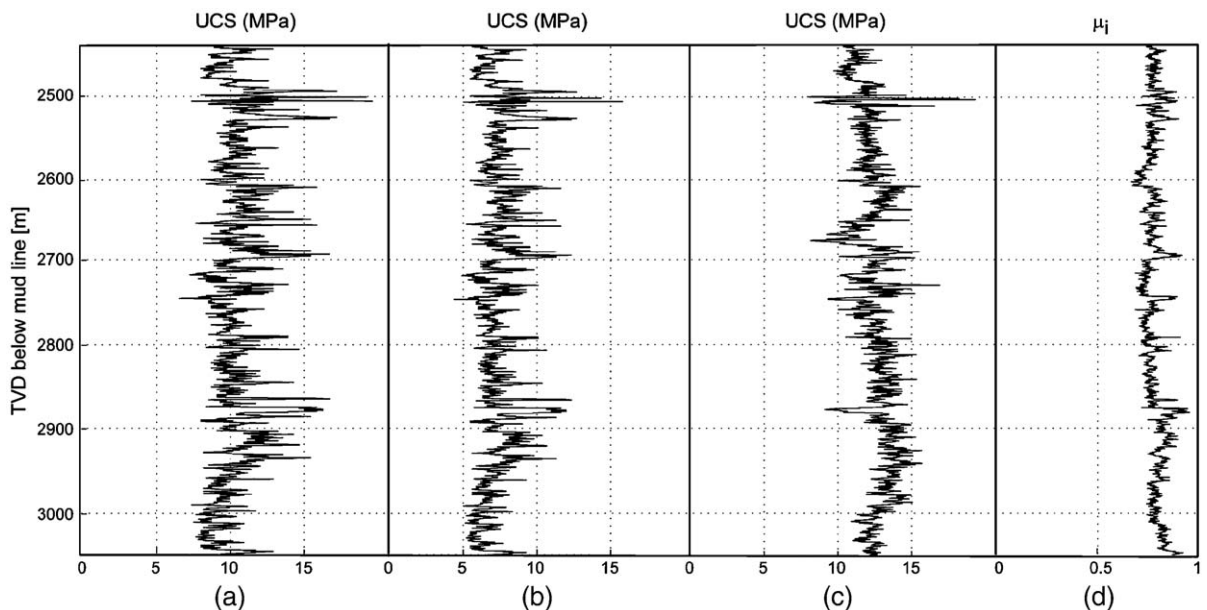

Fig. 8. Unconfined compressive strength (UCS) and internal friction coefficient (μ_i) profile for a shale 2440–3050 m section in a vertical well in the Gulf of Mexico. The UCS profiles in (a), (b) and (c) were determined from geophysical logs using Eqs. (12), (13) and (20), respectively. The internal friction coefficient μ_i in (d) was determined from gamma log using Eq. (32).
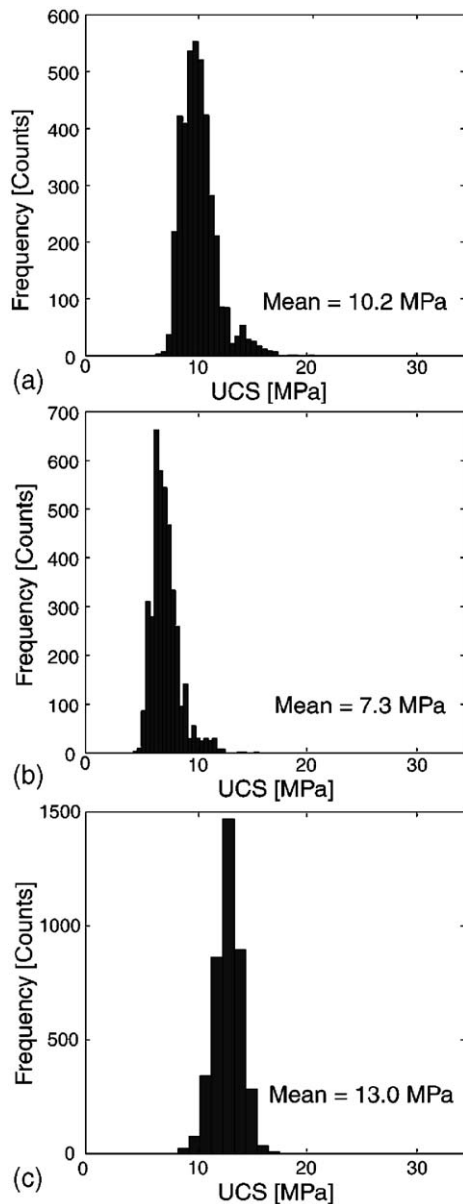
Fig. 9. Histograms of unconfined compressive strength (UCS) values obtained from strength profiles shown in Fig. 8. (a), (b) and (c) here correspond to (a), (b) and (c) in Fig. 8, respectively.

on rock properties may not be universally defined in all types of rock. Shale, for example, may react not only mechanically but also chemically due to the disequilibrium between the chemistry of the pore water and drilling mud. Because the mechanical–chemical interaction of shale with water is not readily quantified, we focus on mechanical effect of saturation only in this study.

The most important effect of saturation is that the dynamic modulus (or velocity) increases as rock is saturated in the context of poroelasticity. Such an effect

can be explained by either Biot flow theory (Biot, 1956) or the squirt flow relation (Mavko and Jizba, 1991), depending on the frequency level used for measurement of modulus. Based on the Biot theory, the saturated bulk modulus (K_{sat}) can be expressed in terms of dry rock properties:

$$\frac{K_{sat}}{K_o - K_{sat}} = \frac{K_{dry}}{K_o - K_{dry}} + \frac{K_{fl}}{\phi(K_o - K_{fl})} \quad (33)$$

where K_{dry} is rock bulk modulus ($K = E/3(1 - 2\nu)$), K_o is bulk modulus of the rock forming grains, and K_{fl} is the bulk modulus of pore fluid. Using Eq. (33), the variation of modulus and transit time before and after saturation can be calculated. Fig. 10 depicts an example of difference in modulus as well as that in transit time between a dry rock and the same rock saturated with typical brine water. Obviously, the effect of saturation is more significant in more porous rocks. For $\phi < 0.25$, the value of Δt decreases by as much as 6 μs/ft, and E increases by as much as 6 GPa, as porosity increases. It appears that the variations of Δt and E for porosity less than 0.25 are not clearly discernable over the scatter in data in Figs. 1–3. For very high porosity rocks ($\phi > 0.25$), the change in the transit time is considerable as rock gets saturated. Thus, if saturated rock specimens had been used for Δt determination in the laboratory, the overall distribution of the data shown in Figs. 1a–3a would have been shifted to the left by a certain amount depending on rock porosity (ϕ) and pore fluid type (i.e. K_{fl}). The result would be to somewhat narrow the difference between UCS_E and UCS_M. Thus, some of the reason of underestimation of UCS can be attributed partly to the fact that the empirical UCS–Δt relations were calibrated using saturated rock samples, whereas the data were measurements (and calculated velocities) on dry rock specimens. Nonetheless, Fig. 10 illustrates the fact that if $\phi < 0.25$, this effect would have extremely small affect on the data presented in Figs. 1–3.

The second effect of saturation is that it often reduces rock strength itself in several possible known mechanisms: reduction of surface energy (Colback and Wiid, 1965), stress corrosion (Atkinson and Meredith, 1987), capillary pressure reduction and chemical effect. While there is no systematic formulation to account for such effects, experiments show that the strength of silicate rocks can drop by as much as 30% due to saturation (Dobereiner and Freitas, 1986). If such effects can be applied to sandstone data shown in Fig. 1, the distribution of data will slightly descend to closer to the empirical relations.

Another uncertainty in the entire analysis is that rock strength data reported in the literature require that
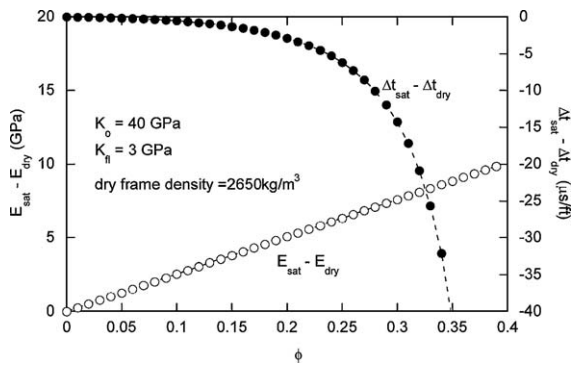
Fig. 10. An example showing difference in Young's modulus (E) and the interval transit time (Δt) between dry and saturated rock, as a function of porosity for a typical rock model parameters (rock forming grain bulk modulus (K_o)=40 GPa, pore fluid bulk modulus (K_{fl})=3 GPa, dry frame density=2650 kg/m^3, and Poisson's ratio=0.25). As porosity increases, the effect of saturation (the increase in Young's modulus and the decrease in the interval transit time) becomes more significant.

laboratory tests have been carried out on samples, which requires relatively good quality samples to facilitate specimen preparation and rock failure experiments. Such samples tend to lack macroscopic fractures, joints and vuggy-shaped pores, which are, in fact, typical of many formations in situ rock. For this reason, laboratory-produced UCS strength data tend to be higher than those in situ. Thus, for a conservative borehole stability analysis, it is always good to note that laboratory-produced data can be used to establish empirical relationships that provide the lower bound of data set.

6. Summary and conclusions

It is clear that a few of the empirical relations discussed above appear to work fairly well for some subsets of the rocks tested in the laboratory. For example, as far as relatively weak rocks are concerned, which are of most interest in cases of wellbore stability, use of Δt with Eqs. (3) and (5) seems to provide a reasonable fit to the strength of weak sands. In addition, Eq. (11) allows one to utilize porosity measurements to estimate weak sand strength when porosity is relatively high ($\phi > 0.1$). With weak shales, Eq. (15) seems to work well when using Δt and Eqs. (20) and (21) seem to work well at relatively high porosity ($\phi > 0.15$). It is more difficult to generalize about limestones and dolomites, but relation (22) appears to fit some of the weaker rocks with high velocity ($\Delta t < 80$) and Eq. (27) appears to allow one to estimate strength from porosity data over

a narrow range of porosities ($0.1 < \phi < 0.25$). While most of other relations do a poor job in fitting measured data for the reasons discussed above, it should not be forgotten that these relations were originally proposed because they fit some subset of data. Therefore, they do work, but not necessarily for the data represented by the published studies available to us. Moreover, a number of the strength–physical property correlations are especially useful in applications related to wellbore stability by providing a lower bound estimate of in situ rock strength. These relations may provide a good first approximation of the lower strength bound when no other information on rock strength is available. It is somewhat obvious, however, that calibration of empirical relations between strength and physical properties is generally required for any correlation to be used with some degree of confidence.

Nomenclature

V_p	P-wave velocity, m/s
Δt	Interval transit time, μs/ft ($1\,\mathrm{μs/ft} = 3.281\,\mathrm{μs/m}$)
E	Young's modulus, GPa
ϕ	Porosity, fraction
V_{clay}	Volume of clay, fraction
ρ	Density, kg/m^3
ν	Poisson's ratio
UCS	Unconfined compressive strength, MPa
Φ	Angle of internal friction, degree
μ_{shale}	Internal friction coefficient of pure shale
μ_{sand}	Internal friction coefficient of pure sand
GR	Gamma ray, API
GR_{shale}	Reference gamma ray of pure shale, API
GR_{sand}	Reference gamma ray of pure sand, API
K_{sat}	Bulk modulus of saturated rock, GPa
K_{dry}	Bulk modulus of dry rock, GPa
K_o	Bulk modulus of rock forming grains, GPa
K_{fl}	Bulk modulus of fluid, GPa

Acknowledgment

References

Atkinson, B.K., Meredith, P.G., 1987. The theory of subcritical crack growth with applications to minerals and rocks. In: Atkinson, B.K. (Ed.), Fracture Mechanics of Rock. Academic Press, London, pp. 111–166.

Batzle, M., Hofmann, R.B., Han, D.-H., Castagna, J., 2001. Fluid and frequency dependent seismic velocity of rocks. Lead. Edge 20, 168–171.

Biot, M.A., 1956. Theory of propagation of elastic waves in a fluid-saturated porous solid: I. Low frequency range and II. higher frequency range. J. Acoust. Soc. Am. 28, 168–191.

Bradford, I.D.R., Fuller, J., Thompson, P.J., Walsgrove, T.R., 1998. Benefits of assessing the solids production risk in a North Sea reservoir using elastoplastic modeling. SPE/ISRM Eurock '98 held in Trondheim, Norway, 8–10 July, 1998, pp. 261–269.

Carmichael, R.S., 1982. Handbook of Physical Properties of Rocks, volume II. CRC Press, Boca Raton.

Cheng, C.H., Johnston, D.H., 1981. Dynamic and static moduli. Geophys. Res. Lett. 8, 39–42.

Colback, P.S.B., Wiid, B.L., 1965. The influence of moisture content on the compressive strength of rocks. Proc. 3rd Canadian Rock Mech. Sympo. 65–83.

Colmenares, L.B., Zoback, M.D., 2002. A statistical evaluation of intact rock failure criteria constrained by polyaxial test data for five different rocks. Int. J. Rock Mech. Min. Sci. 39, 695–729.

Dobereiner, L., Freitas, M.H., 1986. Geotechnical properties of weak sandstones. Geotechnique 36, 79–94.

Drucker, D.C., Prager, W., 1952. Soil mechanics and plastic analysis or limit design. Q. Appl. Math. 10, 157–165.

Ewy, R.T., 1998. Wellbore stability predictions using a modified Lade criterion. Proc. Eurock 98: SPE/ISRM Rock Mechanics in Petroleum Engineering, vol. 1SPE/ISRM Paper, vol. 47251, pp. 247–254.

Fjaer, E., 1999. Static and dynamic moduli of weak sandstones. Rock Mechanics for Industry. Balkema, pp. 675–681.

Fjaer, E., Holt, R.M., Horsrud, P., Raaen, A.M., Risnes, R., 1992. Petroleum Related Rock Mechanics. Elsevier, Amsterdam.

Freyburg, E., 1972. Der Untere und mittlere Buntsandstein SW-Thuringen in seinen gesteinstechnicschen Eigenschaften. Ber. Dtsch. Ges. Geol. Wiss., A; Berlin 176, 911–919.

Golubev, A.A., Rabinovich, G.Y., 1976. Resultaty primeneia apparutury akusticeskogo karotasa dlja predeleina proconstych svoistv gornych porod na mestorosdeniaach tverdych isjopaemych. Prikl. Geofiz. Moskva 73, 109–116.

Gowd, T.N., Rummel, F., 1977. Effect of fluid injection on the fracture behavior of porous rock. Int. J. Rock Mech. Min. Sci. Geomech. Abstr. 14, 203–208.

Handin, J., Hager, R.V., Friedman, M., Feather, J.N., 1963. Experimental deformation of sedimentary rocks under confining pressure: pore pressure tests. Bull. Am. Assoc. Pet. Geol. 47, 717–755.

Horsrud, P., 2001. Estimating mechanical properties of shale from empirical correlations. SPE Drill. Complet. 16, 68–73.

Jizba, D., 1991. Mechanical and Acoustical Properties of Sandstones and Shales, PhD thesis, Stanford University.

Johnston, D.H., Toksöz, M.N., 1980. Ultrasonic P and S wave attenuation in dry and saturated rocks under pressure. J. Geophys. Res. 85, 925–936.

Kwasniewski, M., 1989. Laws of brittle failure and of B–D transition in sandstones. In: Maury, V., Fourmaintraux, D. (Eds.), Rock at Great Depth. A.A.Balkema, Brookfield, VT, pp. 45–58.

Lal, M., 1999. Shale stability: drilling fluid interaction and shale strength. SPE Latin American and Caribbean Petroleum Engineering Conference held in Caracas, Venezuela.

Lama, R.D., Vutukuri, V.S., 1978. Handbook on Mechanical Properties of Rocks, vol. II. Trans Tech Publications, Clausthal, Germany.

Lashkaripour, G.R., Dusseault, M.B., 1993. A statistical study on shale properties; relationship among principal shale properties. Proc.

Conference on Probabilistic Methods in Geotechnical Engineering, Canberra, Australia, 195–200.

Mashinskii, E.I., 2004. Variants of the strain-amplitude dependence of elastic wave velocities in rocks under pressure. J. Geophys. Eng. 1, 295–306.

Mavko, G., Jizba, D., 1991. Estimating grain-scale fluid effects on velocity dispersion in rocks. Geophysics 56, 1940–1949.

Mavko, G., Nur, A., 1979. Wave attenuation in partially saturated rocks. Geophysics 44, 161–178.

McNally, G.H., 1987. Estimation of coal measures rock strength using sonic and neutron logs. Geoexploration 24, 381–395.

Militzer, H., Stoll, R., 1973. Einige Beitrageder geophysics zur primadatenerfassung im Bergbau, Neue Bergbautechnik. Lipzig 3, 21–25.

Moos, D., Zoback, M.D., Bailey, L., 1999. Feasibility study of the stability of openhole multilaterals, Cook Inlet, Alaska. 1999 SPE Mid-Continent Operations Symposium held in Oklahoma City, Oklahoma, 28–31 March 1999, SPE 52186.

Moos, D., Peska, P., Finkbeiner, T., Zoback, M.D., 2003. Comprehensive wellbore stability analysis utilizing quantitative risk assessment. J. Pet. Sci. Eng. 38, 97–110.

Murrell, S.A.F., 1965. The effect of triaxial stress systems on the strength of rocks at atmospheric temperatures. Geophys. J. R. Astron. Soc. 10, 231–281.

Plona, T.J., Cook, J.M., 1995. Effects of stress cycles on static and dynamic Young's moduli in Castlegate sandstone. In: Daemen, Schultz (Eds.), Rock Mechanics. Balkema, Rotterdam, pp. 155–160.

Plumb, R.A., 1994. Influence of composition and texture on the failure properties of clastic rocks. Eurock 94, Rock Mechanics in Petroleum Engineering conference, Delft, Netherlands, pp. 13–20.

Ramana, Y.V., Venkatanarayana, B., 1973. Laboratory studies on Kolar rocks. Int. J. Rock Mech. Min. Sci. Geomech. Abstr. 10, 465–489.

Rzhevsky, V., Novick, G., 1971. The Physics of Rocks. MIR Publ.. 320 pp.

Santarelli, F.J., Detienne, J.L., Zundel, J.P., 1989. Determination of the mechanical properties of deep reservoir sandstones to assess the likelihood of sand production. In: Maury, V., Fourmaintraux, D. (Eds.), Rock at Great Depth. A.A.Balkema, Brookfield, VT, pp. 779–787.

Scott, T.E., Nielsen, K.C., 1991. The effects of porosity on the brittle–ductile transition in sandstones. J. Geophys. Res. 96, 405–414.

Vernik, L., Bruno, M., Bovberg, C., 1993. Empirical relations between compressive strength and porosity of siliciclastic rocks. Int. J. Rock Mech. Min. Sci. Geomech. Abstr. 30, 677–680.

Weingarten, J.S., Perkins, T.K., 1995. Prediction of sand production in gas wells: methods and Gulf of Mexico case studies. J. Petrol. Tech. 596–600.

Wong, S.W., Kenter, C.J., Schokkenbroek, H., van Regteren, J., De Bordes, P.F., 1993. Optimising shale drilling in the Northern North Sea: borehole stability considerations. SPE 26736, Paper Presented at Offshore Europe Conference, Aberdeen, 7–10 September.

Wong, T.-f., David, C., Zhu, W., 1997. The transition from brittle faulting to cataclastic flow in porous sandstones: mechanical deformation. J. Geophys. Res. 102, 3009–3025.

Zoback, M.D., Barton, C.A., Brudy, M., Castillo, D.A., Finkbeiner, T., Grollimund, B.R., Moos, D.B., Peska, P., Ward, C.D., Wiprut, D.J., 2003. Determination of stress orientation and magnitude in deep wells. Int. J. Rock Mech. Min. Sci. 40, 1049–1076.